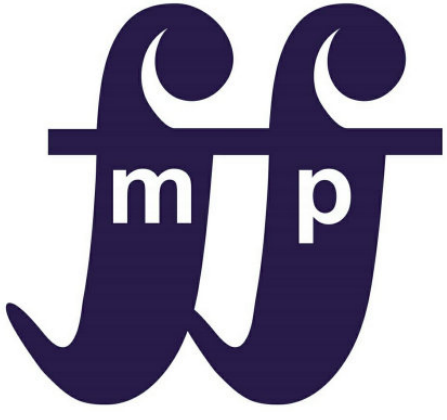
Sensing Particulate Flows using Arrays of Passive Artificial Cilia

[FMFP2022-7656]

Divyaprakash
Amitabh Bhattacharya

Department of Applied Mechanics
Indian Institute of Technology Delhi

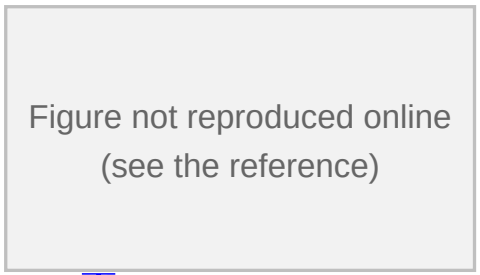
16 December 2022



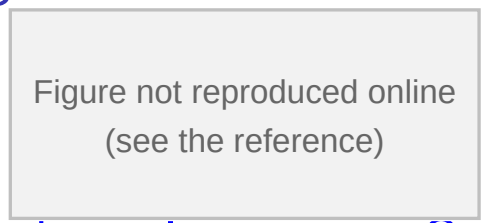


What, Why & How?

What?: Hair like organelles, Cilia are ubiquitous, found in animals and microorganisms, performing various roles



Ovum Transport (Source: Web)



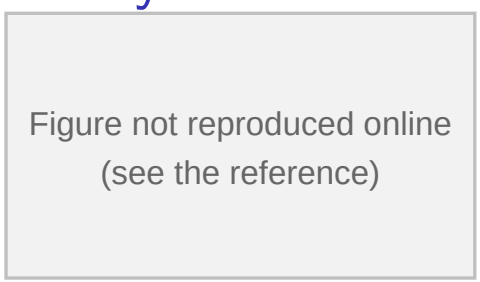
Metachronal waves on Opalina

Reproduced from (Tamm and Horridge 1970)(©2014, The Royal Society.

Why?: Understanding the functionality of cilia can lead to the development of

- Sensors which detect particulate flows and its characteristics
- Design of drug-delivering artificial swimmers

How?: Computational Study

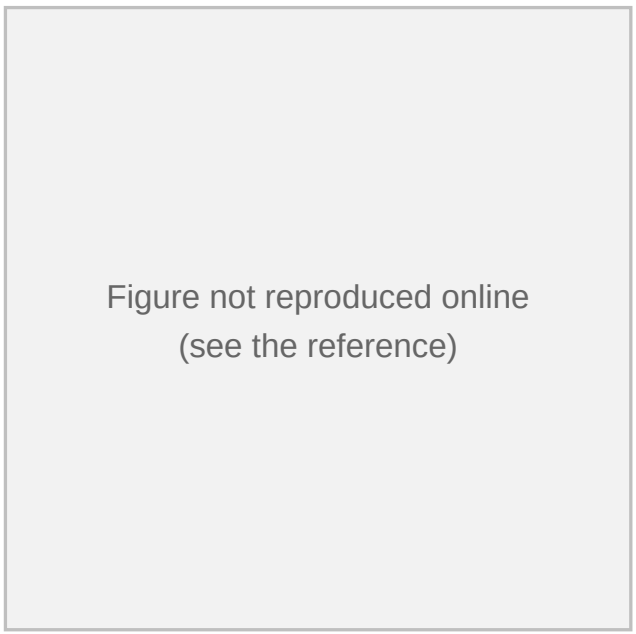


Bhattacharya and Balazs 2013

Research Highlights

Dillon et al. 2007

Study on the transport and mixing of mucus (Non-Newtonian fluid) by cilia arrays in 2D



Transport of a mucus layer

Tripathi, Bhattacharya, and Balazs 2013

Study on size selectivity in suspension feeders by simulating particles' interaction with adhesive artificial cilia

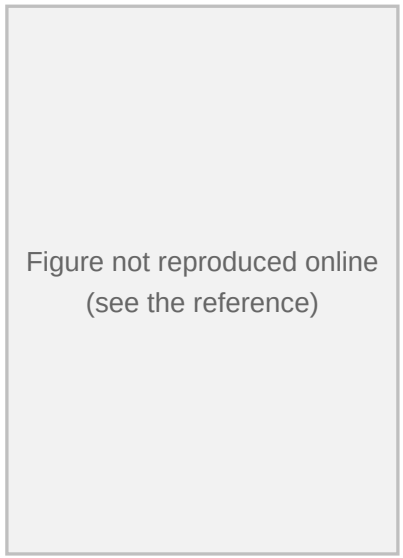


Trajectories of particles as seen projected on the side wall of the channel

Research Highlights

Thomazo et al. 2020

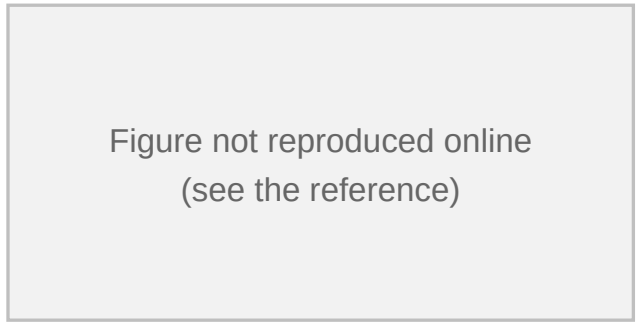
Experimental Study to characterize the size and quantity of particles suspended in fluid subjected to shear flow using artificial passive cilia arrays.



Setup to determine particle's characteristics through cilia deflection

Lin et al. 2021

Development of a machine learning model to predict microcapsules' membrane elasticity and viscosity as they flow in a channel.



Deformation of a micro-capsule flowing through a channel

Motivation

- Most of the studies on cilia particle interactions rely on direct contact.



Bhattacharya and Balazs 2013

- Focus is limited on transport of particles by cilia
- Use of machine learning algorithms can help us predict particle properties given appropriate training.

Objective

Detection of particles' characteristics via their hydrodynamic interactions with non-motile cilia.

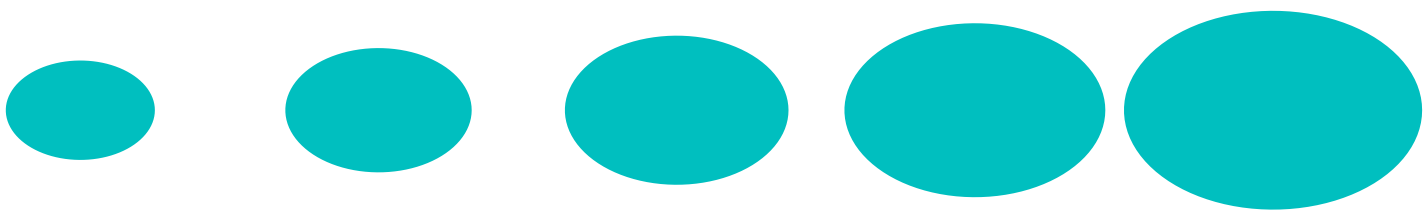
Particle characteristics

Size, shape, area, and location

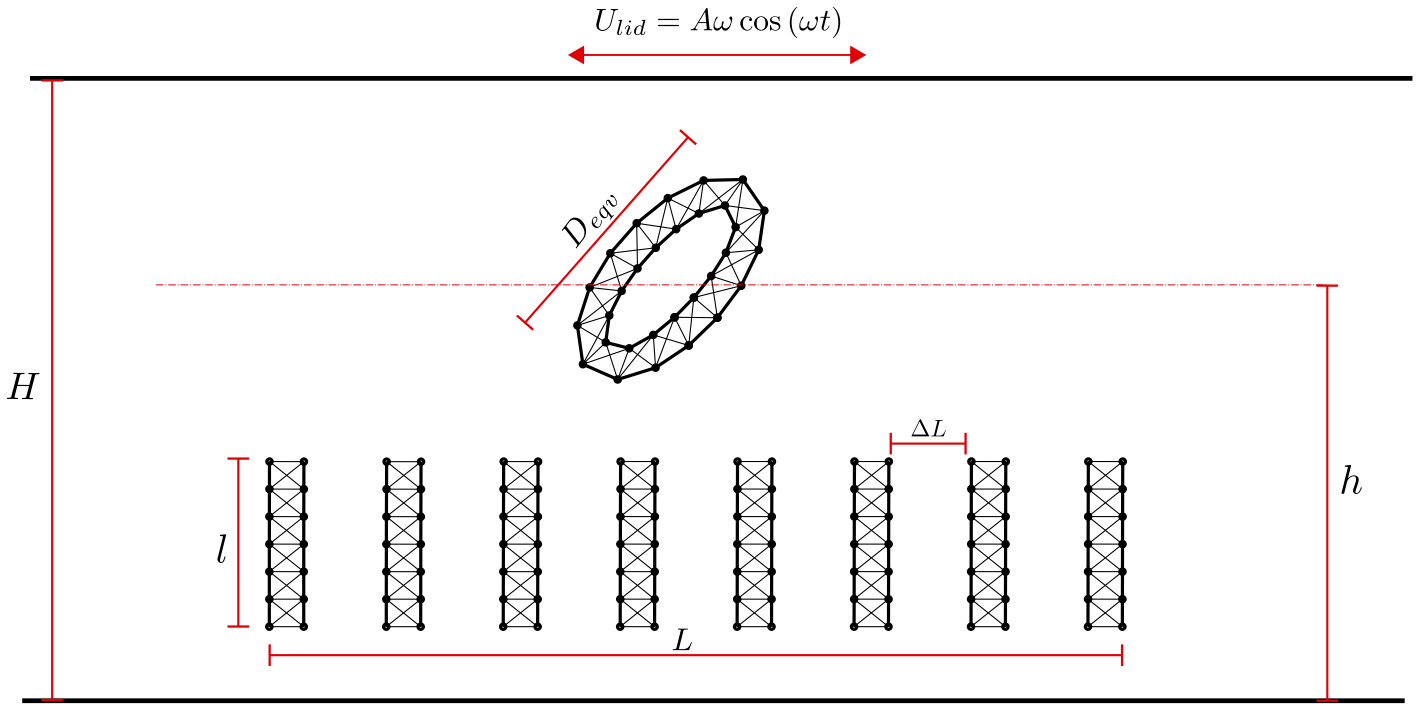
Shape Variation



Size Variation



Cilia-Particle Simulation



Computational Domain

Boundary	Boundary Conditions	
	Velocity	Pressure
Top	No-Slip ($u_x = U_{Top}, u_y = 0$)	Zero-Gradient
Bottom	No-Slip ($\mathbf{u} = 0$)	Zero-Gradient
Left	Zero-Gradient	Constant (P=0)
Right	Zero-Gradient	Constant (P=0)

Dimensionless Numbers

Reynolds number

$$Re = \frac{\text{Inertia Force}}{\text{Viscous Force}}$$

$$Re = HA\omega/\nu$$

Sperm Number

$$S_p = \frac{\text{Viscous Force}}{\text{Elastic Force}}$$

$$S_p = l(4\pi\nu\omega/EI)^{1/4}$$

I, is the area moment of inertia of the cilia cross-section.
The motion of a cilium depends largely on the Sperm number at a low Reynolds number (Bhattacharya and Balazs 2013).

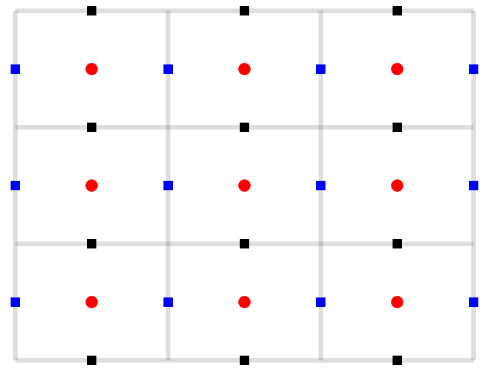
Fluid Flow

Equations

Two-dimensional, unsteady, and incompressible Navier-Stokes equations

$$\nabla \cdot \mathbf{u} = 0$$

$$\frac{\partial \mathbf{u}}{\partial t} + \mathbf{u} \cdot \nabla \mathbf{u} = -\frac{1}{\rho} \nabla p + \nu \nabla^2 \mathbf{u} + \mathbf{f}$$



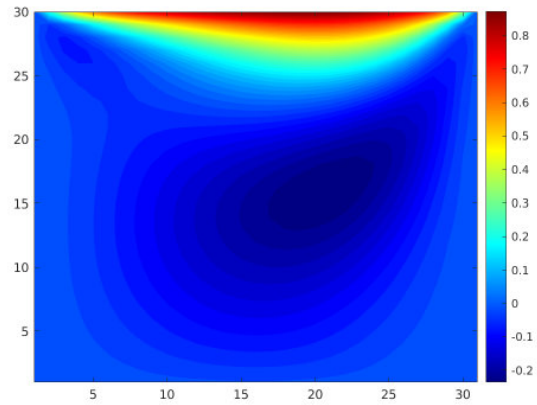
Staggered Grid

Spatial Discretization

Finite difference method (Uniform staggered grid)

Temporal Discretization

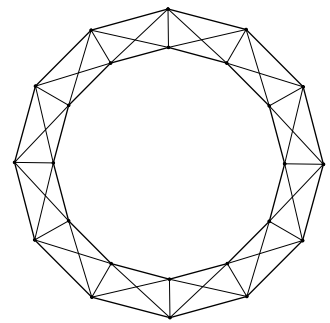
Explicit second-order Runge-Kutta method



Lid driven cavity simulation

Solid Deformation: LSM

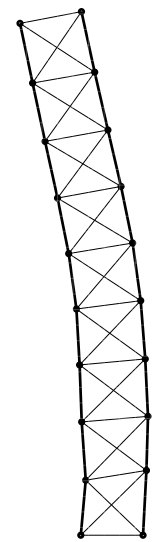
In Lattice Spring Method, a lattice of linear springs joining each node's nearest and next neighbors make up the required elastic structure (Alexeev, Verberg, and Balazs 2005)



The force at each node i is given as,

$$\mathbf{F}_{ij} = -k\left(\frac{|\mathbf{r}_{ij}| - |\mathbf{r}^o_{ij}|}{|\mathbf{r}_{ij}|}\right)\mathbf{r}_{ij}$$

where, $|\mathbf{r}_{ij}|$ is the distance between the nodes with position $\mathbf{r}_i$ and $\mathbf{r}_j$, $|\mathbf{r}^o_{ij}|$ is the distance at equilibrium and k is the spring constant.



Solid Fluid Coupling

Classic immersed boundary method (Peskin 1972)

Force Spreading

$$\mathbf{f}^n(\mathbf{x}_{ij}) = \sum_{i=1}^{N_p} \mathbf{F}_i^n \delta_h(\mathbf{x}_{ij} - \mathbf{X}_i^n)$$

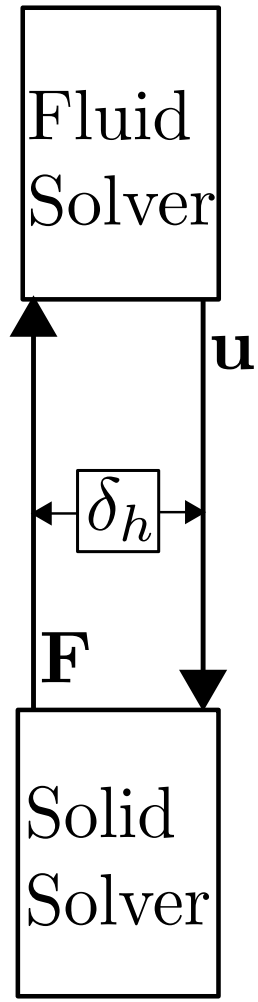
No-Slip Condition (Velocity Interpolation)

$$\frac{\mathbf{X}_i^{n+1} - \mathbf{X}_i^n}{\Delta t} = \mathbf{U}_i^{n+1} = \sum_{i=1}^{N_p} \mathbf{u}^n(\mathbf{x})\, \delta_h(\mathbf{x} - \mathbf{X}_i^n)\, h^2$$

Dirac-δ Function Approximation

$$\delta_h(\mathbf{x}) = h^{-2}\phi\left(\frac{x}{h}\right)\phi\left(\frac{y}{h}\right)$$

$$\phi(r) = \begin{cases} \frac{1}{4}\left(1 + \cos\left(\frac{\pi r}{2}\right)\right), & \text{if } |r| \leq 2 \\ 0, & \text{otherwise} \end{cases}$$

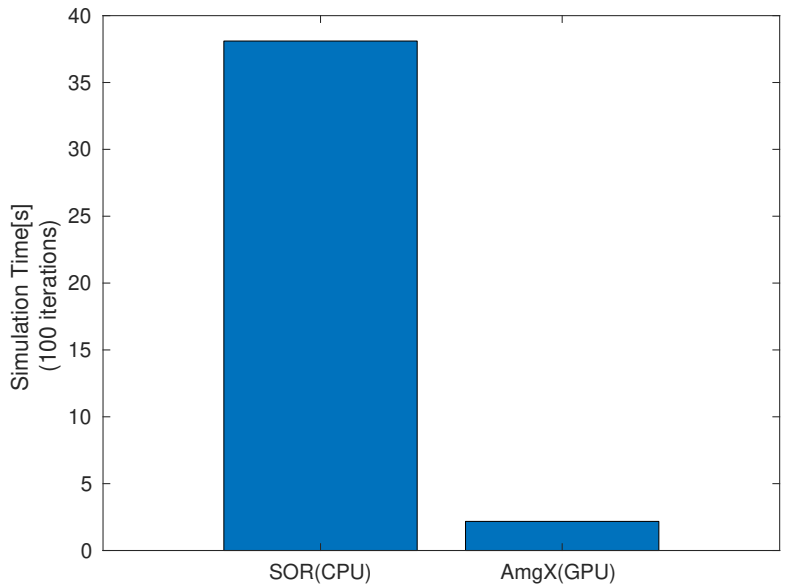


Solver Optimization

Nvidia's open-source library AmgX is used to accelerate the pressure-Poisson solver.

- A Fortran wrapper calling C functions is implemented
- The speedup is attributed to

    1. AMG algorithm's superiority over SOR
    2. GPU's multi-processing capabilities compared to the CPU

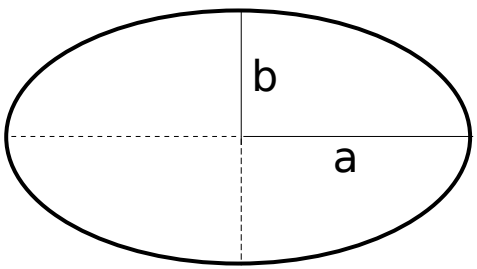


Results and Discussions

Parametric Study

To study the effect of size and shape of particles on cilia tip deflection

Serial No.	Particle Size (Semi-minor Axis) [mm]	Particle Shape (Aspect Ratio)	Actuation Time Period [s]
1	0.25	1	5
2	0.225	1.25	10
3	0.2	1.5	
4	0.175	1.75	
5	0.15	2	



Aspect Ratio = a/b

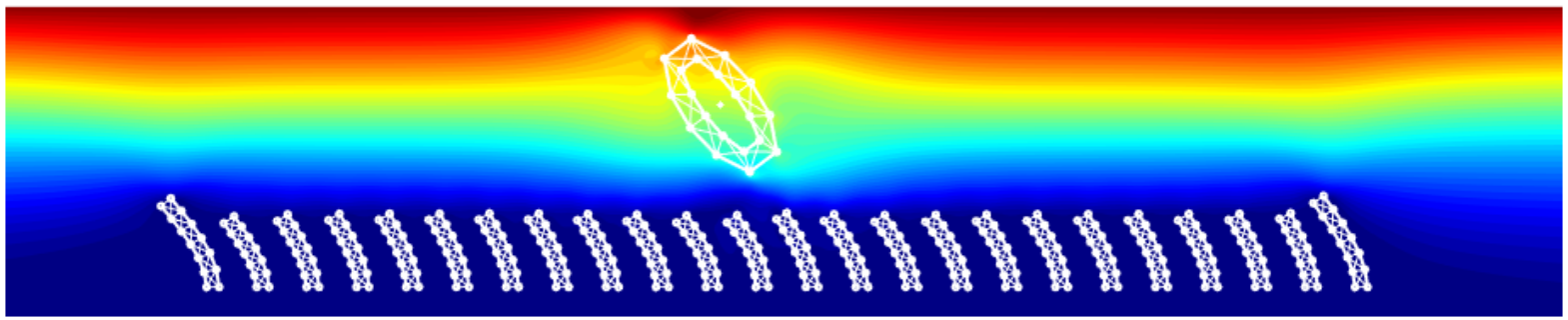
- Low Reynolds numbers of π & 2π
- Low Sperm number of 0.176, &0.148
- Fifty simulation results are obtained using the above parameters.

Simulation Result

Aspect Ratio $= 2$

Semi-minor Axis, b $= 0.25$ *mm*

Actuation Time Period, T $= 10$ *s*



Filled contours of fluid velocity magnitude

Cilia Tip Deflection

Cilia tip deflection at each cilium tip (i) at time-instant t

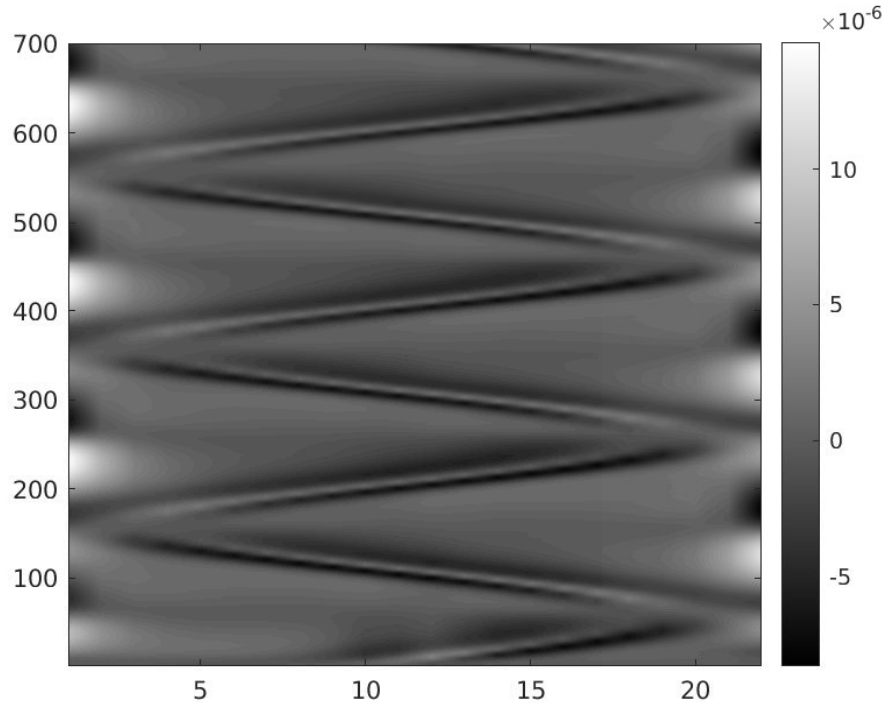
$$\mathbf{r}_i(t) = \langle x_i, y_i \rangle$$

Mean deflection due to lid motion

$$\bar{\mathbf{r}}(t) = \frac{1}{N} \sum_i \mathbf{r}_i(t)$$

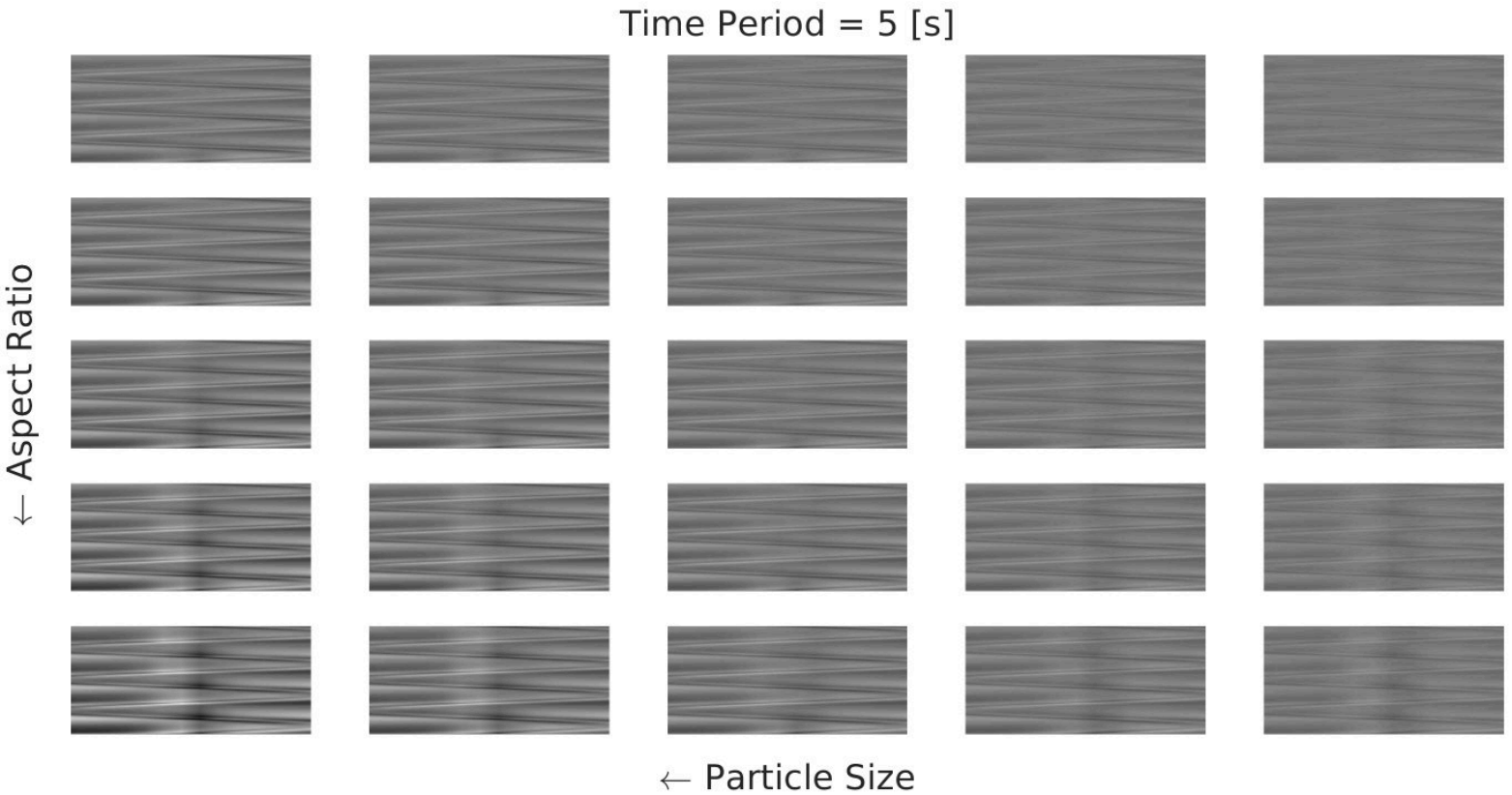
Fluctuations of cilia tip deflection from the mean

$$\mathbf{r'}_i(t) = \mathbf{r}_i(t) - \bar{\mathbf{r}}(t)$$



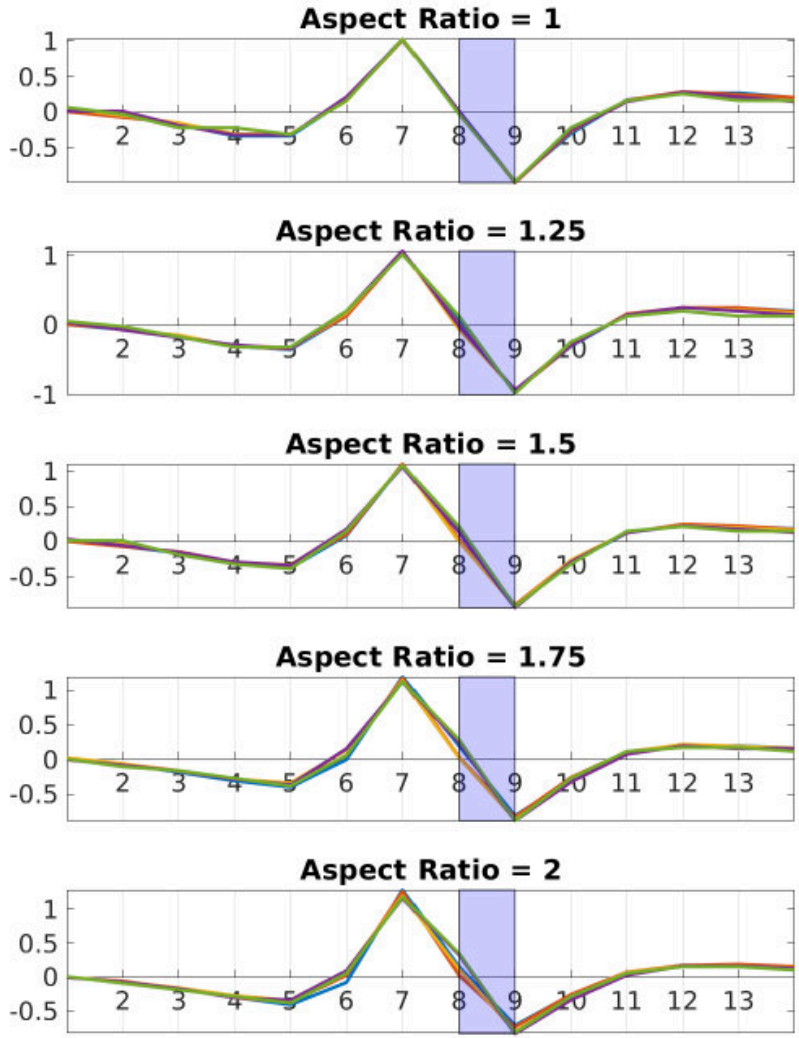
Contours of x'_i on the i-t plane

Size and Shape of Particles



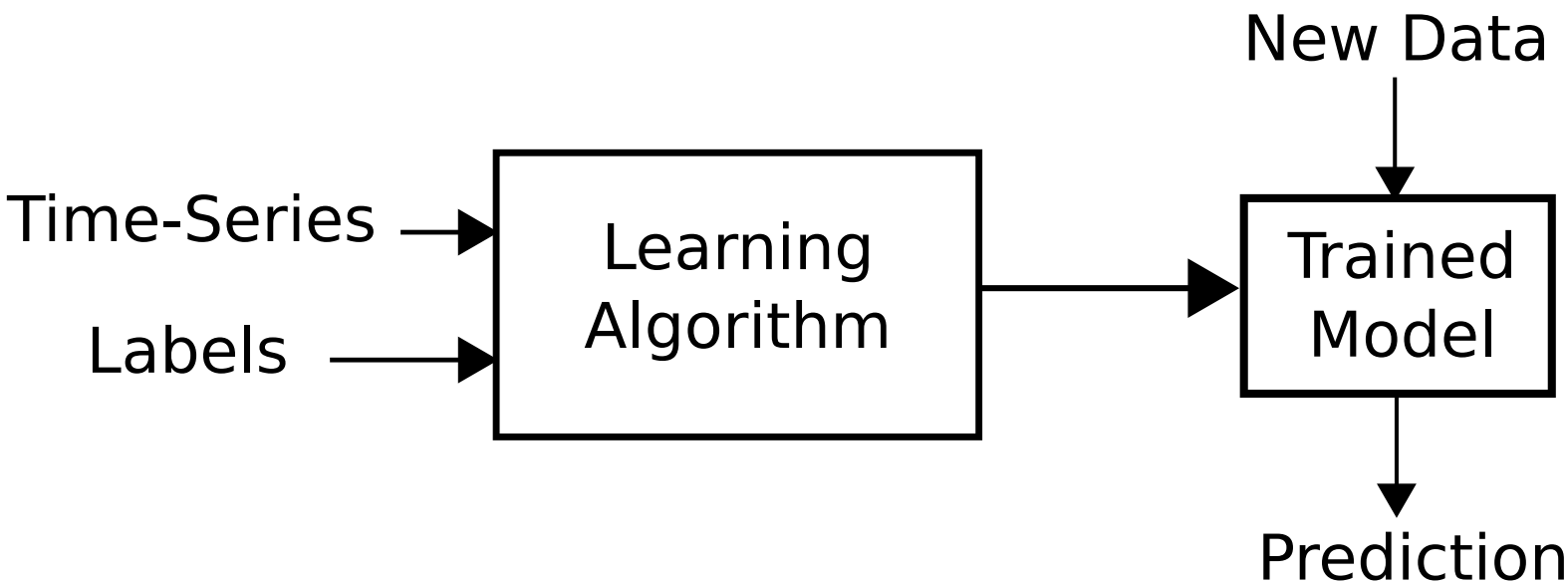
Variation in the contour plots of cilia tip deflection, x_l' with particle size and shape (Re=π & Sp=0.176)

Cilia Tip Deflection



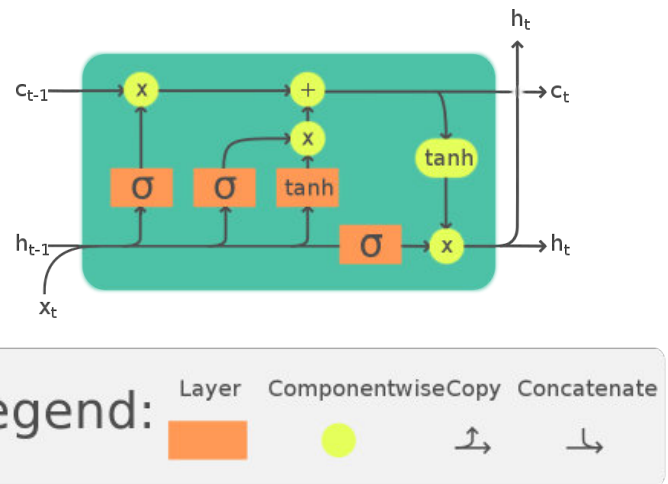
Cilia tip deflection in the wake of the particle

Machine Learning



Long Short Term Memory Network (LSTM)

- Inputs (cilia deflections) to the training algorithm are temporally connected.
- A Recurrent Neural Network (RNN) is able to retain temporal connections in the training examples however they suffer from short term memory.
- LSTM is a type of RNN, but it is capable of learning long term dependencies through it's implementation of "gates".



LSTM cell

Guillaume Chevalier, CC BY-SA 4.0 https://creativecommons.org/licenses/by-sa/4.0 , via Wikimedia Commons

Training

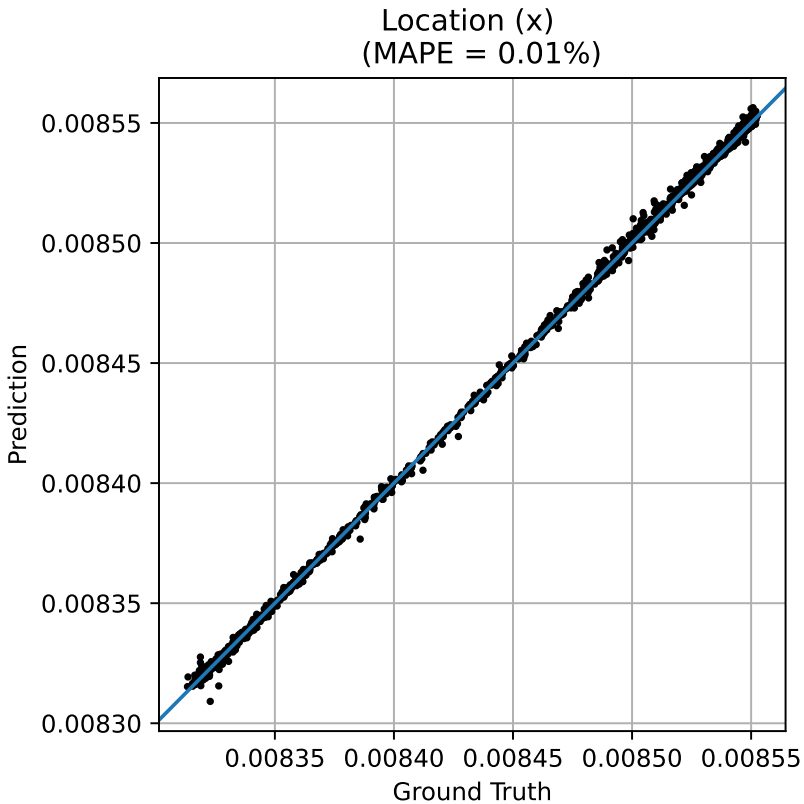
- A multivariate LSTM model is implemented.

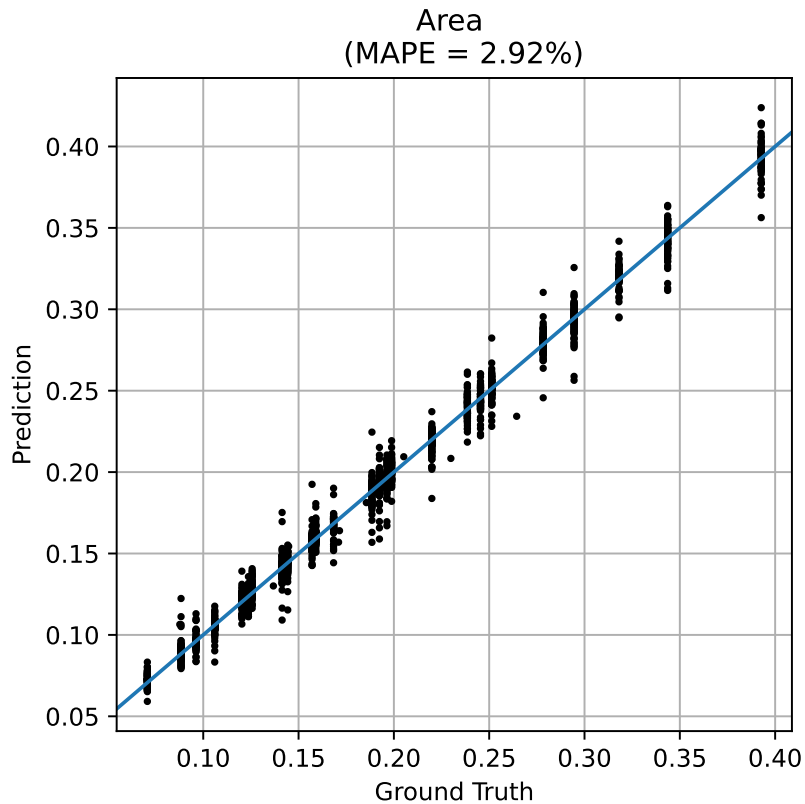
	c_1	c_2	•	•	•	c_M	P
t_1							
t_2							
•							
•							
•							
•							
•							
•							
•							
t_N							

Input data to the model

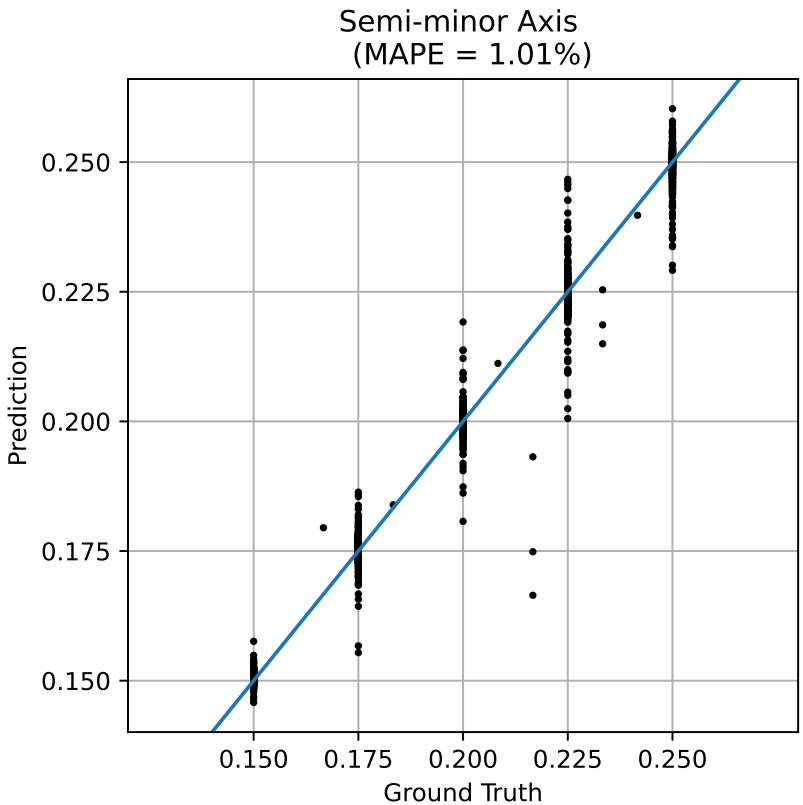
- The final hidden state is fed to a regression layer to predict the particle property.

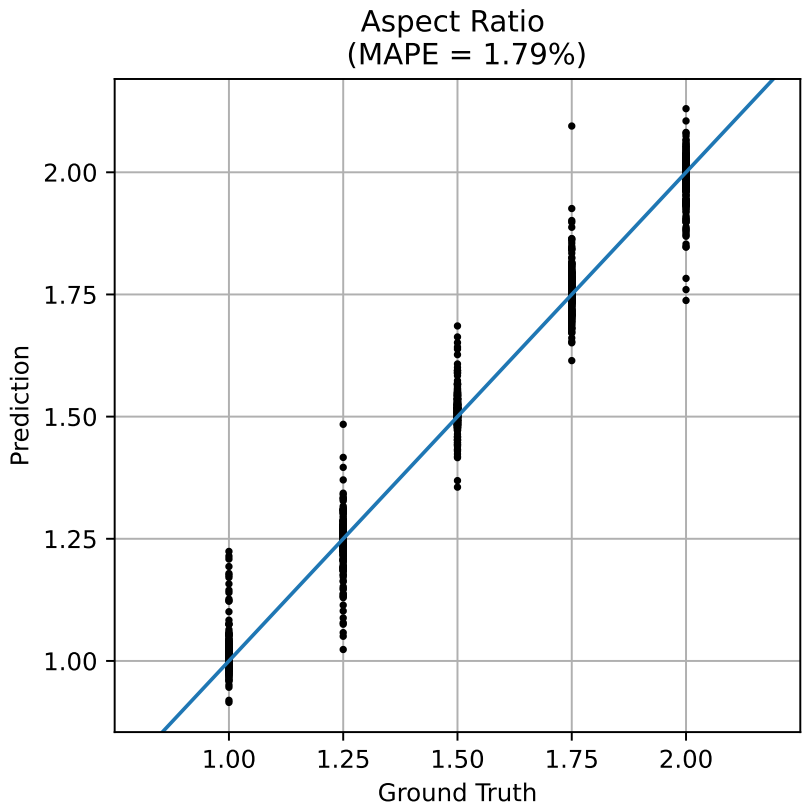
Prediction of Particle Properties (x)





Prediction of Particle Properties (x)





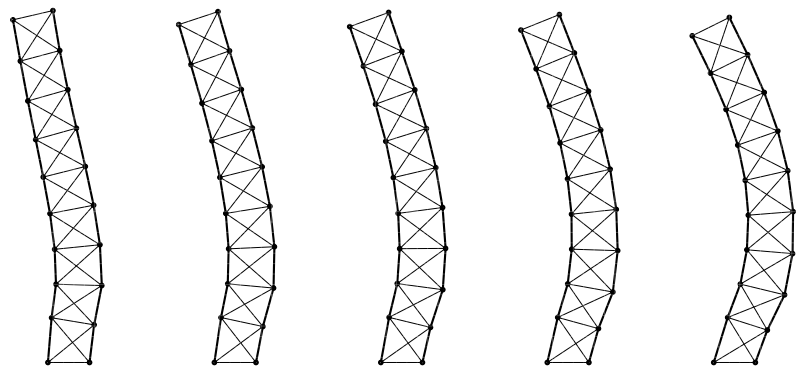
Summary of Predictions

Particle Property	Time Period (s)	Cilia Tip Deflection Component	Mean Absolute Percentage Error (%)
Aspect Ratio	10	x	1.79
		y	4.02
	5	x	4.33
		y	6.16
Semi-minor Axis	10	x	1.01
		y	1.79
	5	x	3.23
		y	3.54
Area	10	x	2.92
		y	3.37
	5	x	4.37
		y	5.09
Location (x)	10	x	0.01
		y	0.02
	5	x	0.02
		y	0.02

Conclusions

1. The cilia tip deflection data can be used to predict particle's
   - location
   - characteristics (size, shape, area)
2. The predictions are most accurate when the inputs to the machine learning model are
   - x-component of cilia tip deflection
   - Low velocity of particle over cilia

Thank You!



References I


Tamm, Sidney L. and George Adrian Horridge (Aug. 1970). "The relation between the orientation of the central fibrils and the direction of beat in cilia of Opalina". In: *Proceedings of the Royal Society of London. Series B. Biological Sciences* 175.1040. Publisher: Royal Society, pp. 219–233. DOI: 10.1098/rspb.1970.0020. URL: https://royalsocietypublishing.org/doi/10.1098/rspb.1970.0020 (visited on 07/22/2022).


Bhattacharya, Amitabh and Anna C. Balazs (Mar. 2013). "Stiffness-modulated motion of soft microscopic particles over active adhesive cilia". en. In: *Soft Matter* 9.15. Publisher: The Royal Society of Chemistry, pp. 3945–3955. ISSN: 1744-6848. DOI: 10.1039/C3SM00028A. URL: https://pubs.rsc.org/en/content/articlelanding/2013/sm/c3sm00028a (visited on 07/24/2022).

References II

- Dillon, R. H. et al. (Feb. 2007). "Fluid Dynamic Models of Flagellar and Ciliary Beating". en. In: *Annals of the New York Academy of Sciences* 1101.1, pp. 494–505. ISSN: 0077-8923. DOI: 10.1196/annals.1389.016. URL: http://doi.wiley.com/10.1196/annals.1389.016 (visited on 10/11/2020).
- Tripathi, Anurag, Amitabh Bhattacharya, and Anna C. Balazs (Apr. 2013). "Size Selectivity in Artificial Cilia–Particle Interactions: Mimicking the Behavior of Suspension Feeders". In: *Langmuir* 29.14. Publisher: American Chemical Society, pp. 4616–4621. ISSN: 0743-7463. DOI: 10.1021/la400318f. URL: https://doi.org/10.1021/la400318f (visited on 07/22/2022).

References III

- Thomazo, Jean-Baptiste et al. (Dec. 2020). "The Ciliated Structure as a Particle Detector". en. In: *arXiv:2012.03832 [cond-mat, physics:physics]*. arXiv: 2012.03832. URL: http://arxiv.org/abs/2012.03832 (visited on 03/17/2021).
- Lin, Tao et al. (2021). "A neural network-based algorithm for high-throughput characterisation of viscoelastic properties of flowing microcapsules". en. In: *Soft Matter* 17.15, pp. 4027–4039. ISSN: 1744-683X, 1744-6848. DOI: 10.1039/D0SM02121K. URL: http://xlink.rsc.org/?DOI=D0SM02121K (visited on 10/05/2021).

References IV

- Alexeev, Alexander, Rolf Verberg, and Anna C. Balazs (Nov. 2005). "Modeling the Motion of Microcapsules on Compliant Polymeric Surfaces". In: *Macromolecules* 38.24, pp. 10244–10260. ISSN: 0024-9297. DOI: 10.1021/ma0516135. URL: https://doi.org/10.1021/ma0516135 (visited on 11/24/2021).
- Peskin, Charles S (Oct. 1972). "Flow patterns around heart valves: A numerical method". en. In: *Journal of Computational Physics* 10.2, pp. 252–271. ISSN: 0021-9991. DOI: 10.1016/0021-9991(72)90065-4. URL: https://www.sciencedirect.com/science/article/pii/0021999172900654 (visited on 07/26/2022).